Generalized Power Series Analysis of Intermodulation Distortion in a MESFET Amplifier: Simulation and Experiment

GEORGE W. RHYNE, STUDENT MEMBER, IEEE, AND MICHAEL B. STEER, MEMBER, IEEE

Abstract —**The design of microwave integrated circuits requires accurate simulation tools capable of predicting a variety of nonlinear distortion effects, including gain compression and intermodulation distortion. This paper uses the recently developed generalized power series analysis to simulate a MESFET amplifier. The simulations are in agreement with experimental results for single-tone and two-tone inputs, thereby validating the analysis method. This analysis is suited to nonlinear microwave circuits having arbitrarily spaced input frequencies.**

I. Introduction

INTEREST IS rapidly growing in the computer-aided design of microwave circuits. While a variety of powerful design tools have been developed for linear circuits, few tools are available for the design of nonlinear analog circuits. In fact, there is currently a large research effort aimed at nonlinear circuit analysis methods. The methods being studied fall into three categories, depending on how the linear and nonlinear circuit elements are handled: time-domain methods, where all elements are analyzed in the time domain (e.g. SPICE [1]); frequency-domain methods, where all elements are analyzed in the frequency domain (e.g. Volterra series techniques [2], [3]); and hybrid methods, which are combinations of time- and frequency-domain techniques including the harmonic-balance methods (e.g. N-FET [4] and HARMONICA [5]). Each of these methods has certain advantages and limitations, which will be briefly discussed. In particular, the suitability of the method to analyzing phenomena such as mixing and intermodulation will be mentioned as this represents an extreme test of the analysis technique.

Time-domain simulators enjoy a wide range of applications, including both analog and digital circuits having either steady-state or transient responses. Several factors, however, limit the applicability of these methods to microwave circuit analysis. Distributed circuits are particularly difficult to model in the time domain. Convergence of the numerical methods is a problem when the circuit contains widely varying time constants or when widely spaced frequency components are present, resulting in lengthy computation times. The time-domain simulation of systems with multifrequency excitation requires multidimensional signal processing to determine intermodulation levels. Both time-domain simulations and multidimensional transform techniques have dynamic range limitations [6] so that small intermodulation levels can be difficult to resolve. Time-domain methods achieve generality at the cost of computation time.

In contrast, frequency-domain methods trade generality for efficiency. These methods determine the steady-state response of a circuit having a small number of sinusoidal inputs. A traditional frequency-domain technique is Volterra series analysis [2], [3]. This technique is ideally suited to multifrequency analysis but is limited in its ability to deal with strong nonlinearities and with large signals. This limitation is due to the algebraic complexity involved with Volterra nonlinear transfer functions of order greater than three.

The hybrid methods are currently enjoying wide popularity. In these methods, the linear circuit elements are analyzed in the frequency domain while the nonlinear elements are analyzed in the time domain. Thus, some of the efficiency of frequency-domain methods is retained but now strong nonlinearities can be handled. The difficulty arises in interfacing the time and frequency domains. This is accomplished using Fourier transform techniques, which requires that the frequencies considered be harmonically related, as in [7], or that in special cases closely spaced frequencies be considered, as in [8]. Thus, these methods are limited in their ability to simulate mixing and intermodulation.

A new frequency-domain technique has recently been developed termed generalized power series analysis (GPSA) [9]–[12]. This method is related to Volterra analysis [13] but is not limited to small signals or to weak nonlinearities. The purpose of this paper is to experimentally verify this technique and to demonstrate its application to a simple MESFET circuit. We present a brief review of GPSA, an outline of the computer simulation used, an explanation of how the transistor is characterized, a description of the experiments, and a discussion of the results.

Manuscript received April 4, 1987; revised July 21, 1987

The authors are with the Department of Electrical and Computer Engineering, North Carolina State University, Raleigh, NC 27695-7911.

IEEE Log Number 8717121.

0018-9480/87/1200-1248$01.00

II. Review of Generalized Power Series Analysis

In this section, we briefly review generalized power series analysis, details of which are presented elsewhere [9]–[12]. A generalized power series is simply a power series with the addition of order-dependent time delays and complex coefficients, for example

$$y(t) = \sum_{l=0}^{\infty} \left[a_l \left\{ \sum_{k=1}^{N} b_k x_k(t - \tau_{k,l}) \right\}^l \right] \tag{1}$$

where $y(t)$ is the output of the system; l is the order of the power series terms; a_l is a complex coefficient; $\tau_{k,l}$ is a time delay that depends on both power series order and the index of the input frequency component; and b_k is a real coefficient. Such an expression can model a wide variety of nonlinear devices [14], [15]. The motivation for expressing the nonlinear elements using such a series is that for an N-component multifrequency input

$$x(t) = \sum_{k=1}^{N} x_k(t) = \sum_{k=1}^{N} |X_k| \cos(\omega_k t + \phi_k) \tag{2}$$

the phasor of the qth component of the output y of radian frequency ω_q is given by [16]

$$Y_q = \sum_{n=0}^{\infty} \sum_{\substack{n_1, \cdots, n_N \\ |n_1| + \cdots + |n_N| = n}} Y_q' \tag{3}$$

where $\omega_q = \sum_{k=1}^{N} n_k \omega_k$, a set of n_k's defines an intermodulation product, and n is the order of intermodulation. Given the generalized power series description (which is a time-domain representation), and a frequency-domain representation of the input (e.g., voltage phasors), formulas are available to calculate the frequency-domain representation of the output (e.g., current phasors) [10], [11], [16]. In addition, formulas are available for calculating the derivatives of the output with respect to the input and for calculating the derivatives of the output with respect to frequency.

The summations of (3) are over the infinite number of intermodulation products (the Y_q''s) yielding the qth output component. Generally when a nonlinear circuit is excited by a finite number of sinusoids, an infinite number of frequency components will be present. In order to analyze such a problem numerically, the number of frequency components considered in the analysis must be truncated.

The formulas just described can be used to analyze nonlinear circuits in a method similar to harmonic balance. (A typical harmonic balance method is described in [7].) In both techniques the circuit is divided into linear and nonlinear subcircuits. Both methods find the steady-state solution by minimizing an objective function with respect to the node voltage phasors. This error function is the sum of the squares of the total currents at each node common to the linear and nonlinear subcircuits, e.g.

$$E = \sum_{p=1}^{M} \sum_{q=1}^{N} |I_{p,q} + I_{p,q}'|^2 \tag{4}$$

where $I_{p,q}$ is the current flowing into the linear subcircuit at node p and frequency q, and $I_{p,q}'$ is the current flowing into the nonlinear subcircuit at node p and frequency q. At steady state the current flowing into the linear subcircuit should be equal and opposite to the current flowing into the nonlinear subcircuit at each frequency, and E should equal zero. Calculation of the error function is done by assuming values for the node voltage phasors and then calculating the current phasors and the error. The voltage estimate is updated, using Newton's method, until the error is reduced to an acceptable level. Here the level of error that is acceptable is dependent on the magnitude of currents flowing in the circuit.

Both harmonic balance and GPSA methods calculate the currents in the linear subcircuit using well-developed frequency-domain circuit techniques. They differ in the calculation of currents in the nonlinear subcircuit. Harmonic balance methods use a Fourier transform to convert the frequency-domain voltages into time-domain signals, and time-domain methods are then used to calculate time-domain currents. In turn, these currents are Fourier transformed into a frequency-domain representation which is used to calculate the harmonic balance error. In GPSA, the frequency-domain voltages are used along with generalized power series representations of the nonlinearities as inputs to formulas that directly calculate the frequency-domain currents. These currents are then used to calculate the error. As transform techniques are not required, GPSA is not limited to harmonically related signals; thus the procedure is termed a spectral balance technique. The following section describes the computer simulations based on this method.

III. Computer Simulations

The simulations described in this paper were done using a program we are developing, called FREDA (FREquency Domain Analysis), based on generalized power series analysis [9], [17]. At this stage of development, FREDA is designed for single MESFET circuits. (Improvements are being made to allow consideration of larger nonlinear circuits.) The nonlinear subcircuit has a fixed topology, shown in Fig. 1, and is used to model the nonlinearities of the MESFET. This topology has been used successfully to model MESFET behavior with other simulation techniques [7], [18], [19]. Each of the nonlinearities in Fig. 1 is described using generalized power series functions of voltage. The linear subcircuit is arbitrary and is specified by the user in a format similar to that for SPICE [1] and TOUCHSTONE [20]. The linear subcircuit contains additional elements needed to model the transistor along with any external circuitry. The user specifies the frequencies to be considered, the dc voltages, and the power levels of the ac sources.

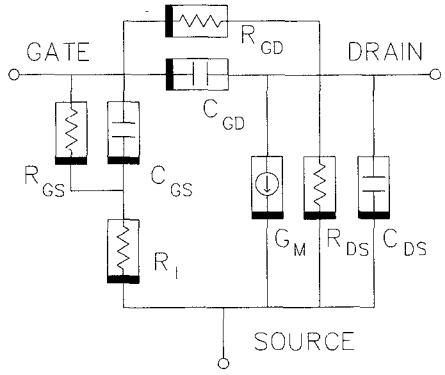

Fig. 1. Circuit used to model the nonlinear behavior of the transistor. Each nonlinear element is represented by a generalized power series.

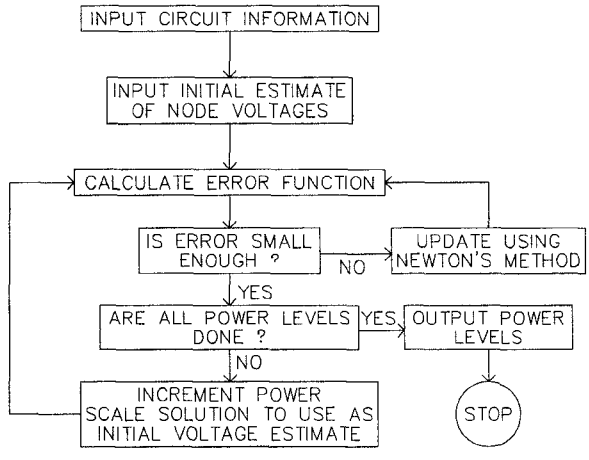

Fig. 2. Flowchart for FREDA.

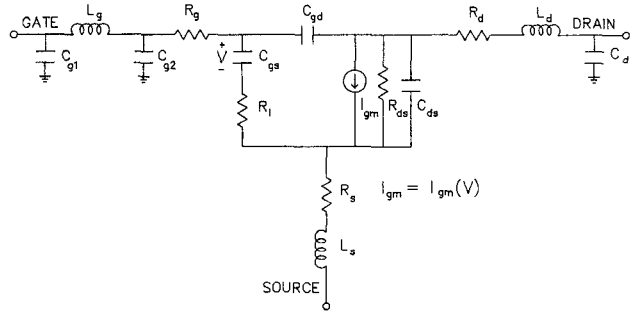

Fig. 3. Complete circuit used to model the transistor.

The operation of FREDA is illustrated in Fig. 2. The circuit to be analyzed is input to FREDA along with information about the frequencies and power levels to be considered (typically a range of input powers is simulated). In addition, FREDA requires an initial estimate of the circuit voltages. This estimate can be made for a low value of input power, where it can be almost arbitrary. This estimate is used to calculate the currents in the linear and nonlinear subcircuits and the derivatives of the currents with respect to the node voltages. The currents are used to calculate the error function and the derivatives are used to calculate the Jacobian. The voltage estimate is updated using Newton's method. This is continued until the error is reduced to an appropriate level. The input power level is then incremented and the previous solution, appropriately scaled, is used as the next initial estimate. The level of error that is acceptable is determined as a fraction of the dc drain–source current, as in [7]. In the simulations described in this paper, the ratio of the square root of the current error (4) to the dc drain–source current is at most 10^{-4}.

The circuit of Fig. 3 (with 50-Ω source and load impedances and bias circuitry added) was simulated using FREDA. For these simulations no matching circuits were used and simulations were performed for the case of a single-tone input as well as for two input tones. The following section describes the characterization of a transistor for use in the simulations.

IV. Device Characterization

The device used here is a low-noise, medium-power GaAs MESFET (Avantek AT8250). While the nonlinear behavior of the transistor is modeled by the circuit of Fig. 1, the complete transistor model, including parasitics and other linear elements, is shown in Fig. 3. In the simulations presented here only G_m, C_{ds}, C_{gs}, and R_{ds} of Fig. 1 were taken to be nonlinear. The linear element values and the generalized power series representations were developed from dc and small-signal microwave measurements assuming the device to be quasi-static [21]. The procedure used to determine the model parameters is illustrated in Fig. 4.

The magnitude of the transconductance G_m was found from dc measurements of the drain current at varying gate–source voltages with the drain–source voltage fixed at the chosen operating point ($V_{ds} = 3$ V). Small-signal s parameters were measured over the frequency range 0.5–15.0 GHz at various bias voltages, including zero bias (i.e., $V_{ds} = V_{gs} = 0$ V). With zero drain–source voltage, the equivalent circuit becomes the circuit shown in Fig. 5, which is useful in determining the various parasitic elements because the model for the transistor has three fewer elements to be optimized [22], [23]. TOUCHSTONE [20] was used to optimize the circuit of Fig. 5 to match the measured zero-bias s parameters over the frequency range 0.5–10 GHz. (The values of R and C which model the channel at zero bias were also optimized, although their values are not used in the simulations.) With the linear elements determined, the model of Fig. 3 was then optimized to match the measured s parameters at each bias setting, resulting in a table of nonlinear element values as a function of bias voltage. Figs. 6 and 7 compare the measured s parameters and the s parameters of the transistor model. Because FREDA cannot currently handle multidimensional nonlinearities, the drain–source current must be modeled as a component dependent only on the gate–source voltage and a component dependent only on the drain–source voltage. This restriction results in a compromise in the selection of values for G_m and R_{ds} between the best fit at the operating point versus the best fit over a range of voltage. The result is the imperfect fit between the model and the measured s parameters, particularly S_{22}.

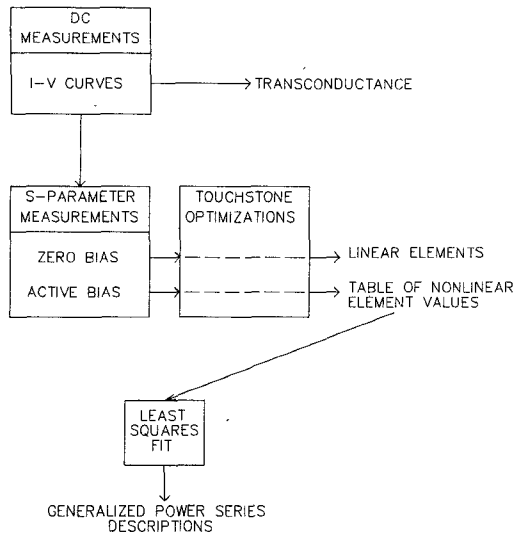

Fig. 4. Procedure used to develop the transistor model.

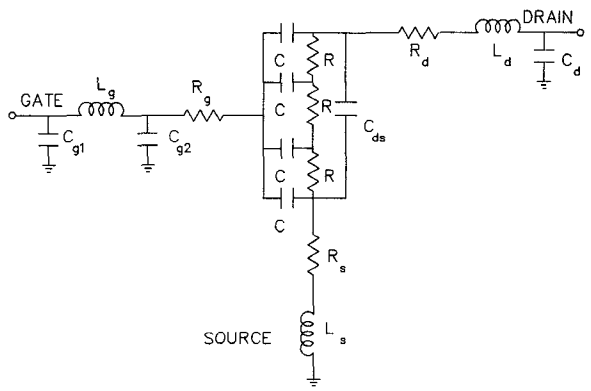

Fig. 5. Circuit used to model the transistor at zero bias.

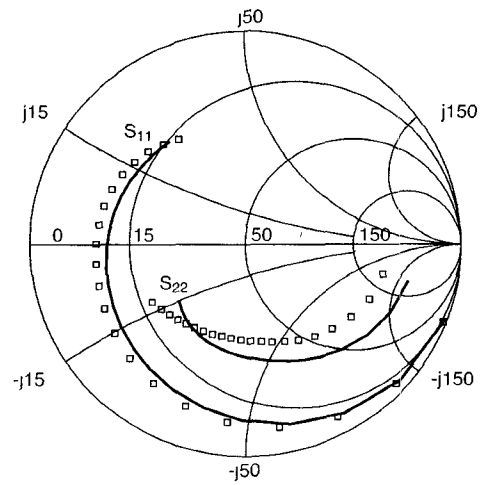

Fig. 6. Comparison of measured values (points) and simulated values (solid lines) of S_{11} and S_{22} over the frequency range 0.5–10.65 GHz at the bias point $V_{ds} = 3.0$ V, $V_{gs} = -0.1$ V.

The nonlinear simulation requires that the nonlinear element values be described by generalized power series in voltage. A least-squares routine was used to fit power series to the data determined from the TOUCHSTONE optimizations. The power series are of the following form:

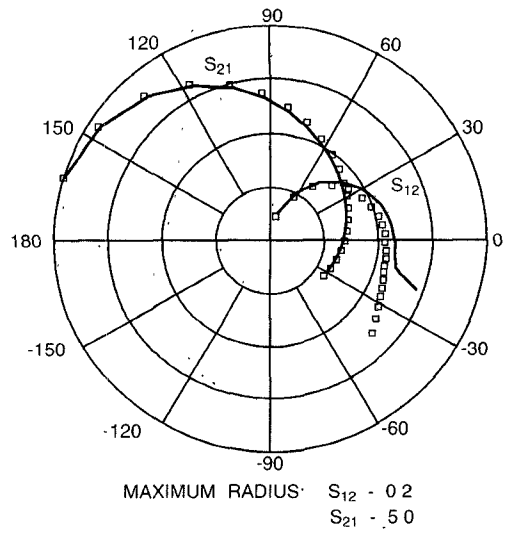

Fig. 7. Comparison of measured values (points) and simulated values (solid lines) of S_{12} and S_{21} over the frequency range 0.5–10.65 GHz at the bias point $V_{ds} = 3.0$ V, $V_{gs} = -0.1$ V.

TABLE I
POWER SERIES COEFFICIENTS USED AS INPUTS TO THE SIMULATIONS

series	order of coefficient							
	0	1	2	3	4	5	6	7
I_{gm}	266e-1	696e-1	275e-1	-.340e-1	211e-1	400e-1	-.212e-1	-.224e-1
C_{gs}	656e-12	387e-12	154e-12	.897e-12	614e-12			
C_{ds}	386e-12	-.289e-12	138e-12	-.290e-13	231e-14			
I_{rds}	-.361e-1	672e-1	-.717e-1	447e-1	-.161e-1	331e-2	-.369e-3	.169e-4

These are the functions described by (5)–(8) and plotted in Figs. 8 and 9. The simulations require functions for charge as a function of voltage instead of capacitance. The series for C_{gs} and C_{ds} are modified as explained in the text.

the drain–source current component dependent on the gate–source voltage

$$I_{gm} = g_{m0} + g_{m1}V'_{gs} + g_{m2}V'^2_{gs} + \cdots \tag{5}$$

where $V'_{gs} = V_{gs}e^{-j\omega\tau}$ and $g_m = \partial I_{gm}/\partial V_{gs}$; the drain–source current component dependent on the drain–source voltage

$$I_{rds} = r_{ds0} + r_{ds1}V_{ds} + r_{ds2}V^2_{ds} + \cdots \tag{6}$$

where $G_{ds} = \partial I_{rds}/\partial V_{ds}$; the gate–source capacitance

$$C_{gs} = C_{gs0} + C_{gs1}V_{gs} + C_{gs2}V^2_{gs} + \cdots \tag{7}$$

and the drain–source capacitance

$$C_{ds} = C_{ds0} + C_{ds1}V_{ds} + C_{ds2}V^2_{ds} + \cdots. \tag{8}$$

In circuit simulations the nonlinear capacitors must be described by equations of charge as a function of voltage instead of capacitance. Equations (7) and (8) are easily converted by integrating with respect to voltage, e.g.

$$Q(v) = \int C(v)\,dv. \tag{9}$$

The current through the capacitor is found by taking the time derivative of the charge. If I_k and Q_k are phasor

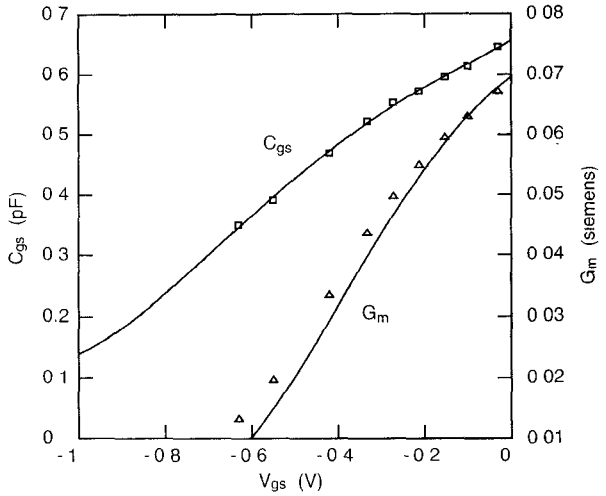

Fig. 8. Optimized values of the gate–source capacitance C_{gs} and the transconductance G_m as a function of gate–source voltage. The points are the optimized values and the curves are the power series representations.

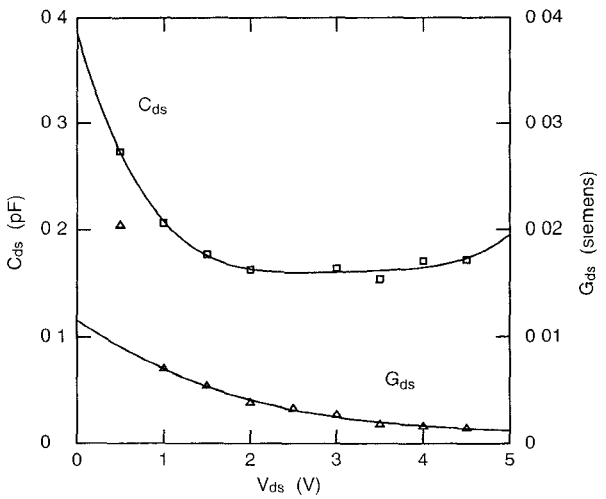

Fig. 9 Optimized values of the drain–source capacitance C_{ds} and the drain–source conductance G_{ds} as a function of drain–source voltage. The points are the optimized values and the curves are the power series representations.

components, with radian frequency ω_k, of current and charge, then $I_k = j\omega_k Q_k$. Thus the current flowing through the capacitor can be expressed in terms of a generalized power series of voltage

$$i_c = j\omega\left(q_1 V + q_2 V^2 + \cdots\right) \tag{10}$$

where ω, the radian frequency of a component of i_c, is not unique. The values of the power series coefficients corresponding to (5)–(8) are summarized in Table I. It should be noted that the series are functions of one variable only and that while expressions for capacitance as a function of voltage are input to the simulations, these are converted to expressions of charge with respect to voltage for simulation purposes. Although some of these elements are best described by functions of both V_{gs} and V_{ds}, only elements that are nonlinear functions of a single variable can be simulated using the current software. Work is in progress

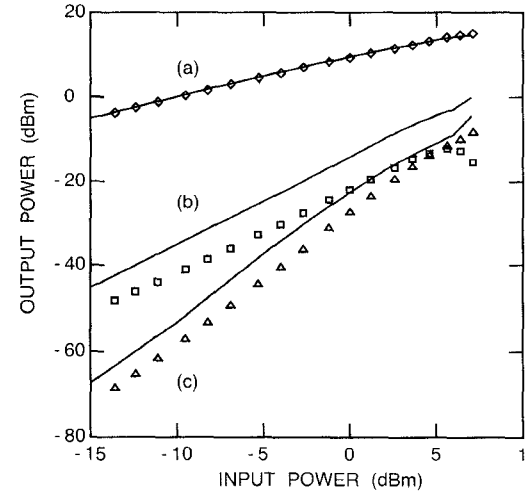

Fig. 10. Results of the single-tone test. Power output in (a) the fundamental at 3 GHz, (b) the second harmonic, and (c) the third harmonic are shown as a function of input power. The points are measurements and the curves are simulated results.

to extend these techniques to multidimensional functions. Figs. 8 and 9 show the optimized values of G_m, C_{gs}, G_{ds}, and C_{ds} compared to their power series representations.

V. Experiment

The transistor was placed in an Avantek test fixture and bias was applied through two broad-band bias tees so that $V_{ds} = 3$ V and $V_{gs} = -0.1$ V. The power input to the device was computer controlled using a p-i-n diode attenuator. The power output was measured using a spectrum analyzer, which was also computer controlled. The input power was incremented in steps and the power was measured at all frequencies of interest.

For the single-tone test, an input frequency of 3 GHz was used and the output power was measured at 3, 6, and 9 GHz. The input power was varied from -35 dBm to 10 dBm. In Fig. 10 the results of the simulation with one input tone are compared to the experimental results. The simulation is continued until the gain is compressed by 3 dB from its small-signal value of 10.1 dB. Experimentally, the small-signal gain was observed to be approximately 10 dB and the power output in the fundamental saturated at 16 dBm. Shown are the fundamental and first two harmonics.

For the two-tone intermodulation test, the transistor was again biased at $V_{ds} = 3$ V and $V_{gs} = -0.1$ V. Two equal-amplitude signals were input, one at 2.35 GHz and one at 2.40 GHz. The input power was varied from -35 dBm to 5 dBm, and the output power was measured at the fundamental frequencies, their harmonics, and the third-order intermodulation frequencies. (The frequencies and power levels used were chosen entirely for experimental convenience and not for ease of simulation.) The results of the two-tone intermodulation test are shown in Fig. 11. The power output in one of the input tones (2.35 GHz) is shown along with the power output in one of the third-order intermodulation frequencies (2.3 GHz).

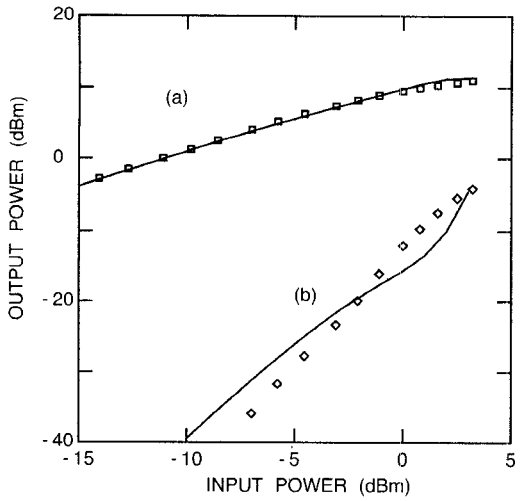

Fig. 11. Results of the two-tone test. Power output in (a) one of the fundamentals at 2.35 GHz and in (b) one of the third-order intermodulation frequencies at 2.3 GHz is shown as a function of input power. The points are measurements and the curves are simulated results.

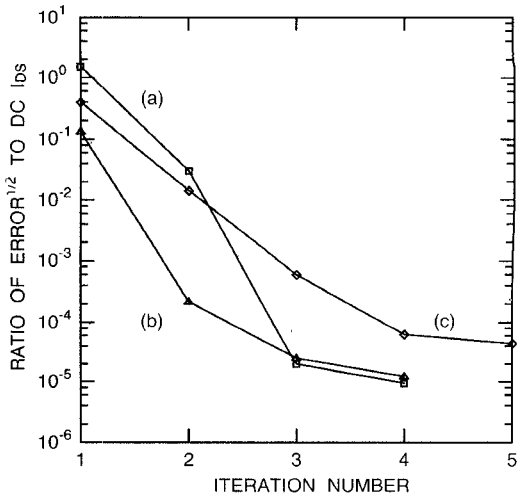

Fig. 12. The square root of the error of (4) divided by the dc drain–source current for the two-tone simulation as a function of the iteration number. (a) Simulation with −10 dBm input power. The initial estimate for the node voltages is arbitrary (except for dc, which is set to the bias level). This solution was used to obtain the initial estimate for (b) a simulation with −5 dBm input power. The process was repeated for (c) a simulation with 0 dBm input power.

VI. Discussion

In the single-tone and two-tone test results in Figs. 10 and 11, the predicted powers output at the fundamental frequency are seen to be in excellent agreement with the experimental results. The agreement for the power output at the harmonic frequencies shown in Fig. 10 is not as good. This is believed to be due to the neglect of forward conduction through the gate and to the two-dimensional character of the drain–source current, which is not adequately modeled here. The third-order intermodulation product is accurately predicted, however, as shown in Fig. 11.

Fig. 12 shows the magnitude of the square root of the current error (4) divided by the dc drain–source current as a function of the iteration number for several points in the two-tone simulation. Typically, FREDA converges in less than ten iterations per point and often fewer than five iterations are required. Indeed, if the nonlinear elements are actually linear, convergence is obtained after one or two iterations. The method is very efficient for weakly nonlinear circuits or when the applied signals are small. Computational effort increases only when the nonlinearity is significant.

It is interesting to compare the performance of FREDA to the harmonic balance simulator reported in [7]. Curtice uses harmonic balance to simulate a single MESFET amplifier with two tones input. In [7] the simulated intermodulation distortion results are within a few dB of the experimental results, comparable to the results presented here in Fig. 11. The computation times are significantly different. Curtice reports a typical execution time of 8 min on a VAX 11/780 with a floating-point accelerator. The simulations reported here require 60–90 s on a MicroVAX II running ULTRIX 1.2. Another difference is that the simulations using FREDA do not require the frequencies to be harmonically related, as is required in the harmonic balance methods.

In addition to calculating output powers at all the frequencies considered, FREDA provides information about the behavior of the nonlinear elements. This information can be used to calculate the effective value of the elements at the fundamental frequency as a function of input power. When the steady-state solution has been found, FREDA provides the currents through the nonlinear elements and the voltages across the elements at all of the frequencies used in the simulation. Dividing the fundamental component of the voltage across an element by the fundamental component of the current through the element gives a quantity which can be regarded as the effective large-signal impedance seen at the fundamental frequency. The calculated impedances can then be interpreted as resistors, capacitors, or inductors, as required.

Effective element values, as seen at the fundamental, were calculated for each nonlinear component of the MESFET model (see Fig. 1) using the procedure described above. In Fig. 13 the effective value of the transconductance (G_m) as a function of incident power is plotted and is seen to decrease by about 25 percent over the range of input power considered.

More interesting effects are noticed in the large-signal behavior of the gate–source capacitance (C_{gs}). As the power input to the transistor is increased, the current through the nonlinear capacitor begins to have a component that is in phase with the voltage across the capacitor. This is a parametric effect and can be modeled at the fundamental as a resistance in parallel with a capacitance. This resistance represents the power converted from the fundamental to another frequency. Fig. 14 shows the values of the parallel resistor and capacitor needed to predict the large-signal behavior of C_{gs} as a function of input power. The effective capacitance increases by about 8 percent while the effective resistance decreases by a factor

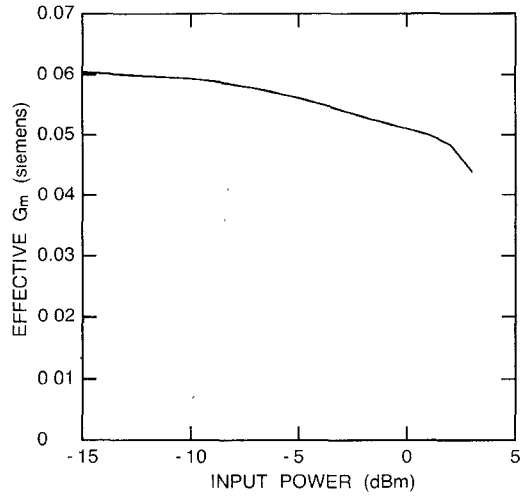

Fig. 13. The effective value of the transconductance at the fundamental frequency as a function of the input power for the two-tone simulation.

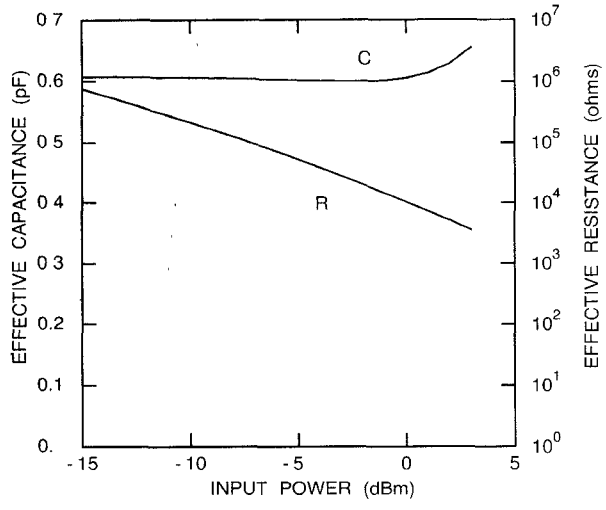

Fig. 14. The values of the parallel resistor and capacitor needed to model the large-signal behavior of C_{gs} at the fundamental frequency as a function of input power for the two-tone simulation.

of 200. This has significant implications for the phase performance of the device.

VII. Conclusions

In this paper, we have verified the generalized power series analysis simulation technique for a MESFET amplifier circuit with a single-tone input as well as for a two-tone intermodulation test. This technique is significant because it can be used to simulate nonlinear circuits having large-signal multifrequency inputs where the separation of the signal frequencies is arbitrary. The method provides for accurate calculation of the Jacobian, which results in excellent convergence properties. Because Fourier transforms are not needed and because each frequency component is calculated separately, a large dynamic range is achieved.

This method requires that the nonlinearities be expressed as generalized power series functions of a single variable. A wide range of nonlinear elements can be described in this way and an implementation allowing multivariable functions is under development. This will allow more accurate modeling.

Generalized power series analysis is an attempt to fill a void that currently exists in CAD software for the analysis of nonlinear microwave circuits. By simulating circuits having nonharmonically related input frequencies, it makes a significant contribution. This analysis can also be used in simulating oscillators, since derivatives of current with respect to frequency can also be calculated when using generalized power series representations. The simulation of oscillators is particularly difficult using currently available software.

Acknowledgment

The authors would like to acknowledge the assistance of W. Lawrence in the measurement of device s parameters.

References

[1] L. W. Nagel and D. O. Pederson, "SPICE (Simulation Program with Integrated Circuit Emphasis)," University of California, Electronics Research Laboratory Memorandum ERL-M382, Apr. 12, 1973.

[2] R. A. Minasian, "Intermodulation distortion analysis of MESFET amplifiers using Volterra series representation," *IEEE Trans. Microwave Theory Tech.*, vol. MTT-28, pp. 1–8, Jan. 1980.

[3] C. L. Law and C. S. Aitchison, "Prediction of wide-band power performance of MESFET distributed amplifiers using the Volterra series representation," *IEEE Trans. Microwave Theory Tech.*, vol. MTT-34, pp. 1308–1317, Dec. 1986.

[4] W. R. Curtice and M. Ettenberg, "N-FET, A new software tool for large-signal GaAs FET circuit design," RCA Rev., vol. 46, pp. 321–340, Sept. 1985.

[5] K S. Kundert and A Sangiovanni-Vincentelli, "Simulation of nonlinear circuits in the frequency domain," *IEEE Trans. Computer-Aided Design*, vol. CAD-5, pp. 521–535, Oct. 1986.

[6] D. Hente and R. H. Jansen, "Frequency domain continuation method for the analysis and stability investigation of nonlinear microwave circuits," *Inst. Elec. Eng.*, vol. 133, pt. H, pp. 351–362, Oct. 1986.

[7] W. R. Curtice, "Nonlinear analysis of GaAs MESFET amplifiers, mixers, and distributed amplifiers using the harmonic balance technique," *IEEE Trans. Microwave Theory Tech.*, vol. MTT-35, pp 441–447, Apr. 1987.

[8] R. J. Gilmore and F. J. Rosenbaum, "Modelling of nonlinear distortion in GaAs MESFET's," in *IEEE MTT-S Int. Microwave Symp. Dig.*, 1984, pp. 430–431.

[9] G. W Rhyne and M. B. Steer, "A new frequency domain approach to the analysis of nonlinear microwave circuits," in *IEEE MTT-S Int. Microwave Symp. Dig.*, 1985, pp. 401–404.

[10] G. W. Rhyne, M. B. Steer, and B. D. Bates, "Analysis of nonlinear circuits driven by multi-tone signals using generalized power series," in *IEEE Int. Symp. Circuits Syst. Dig.*, 1987, pp. 903–906.

[11] G. W. Rhyne, M. B. Steer, and B. D. Bates, "Frequency domain nonlinear circuit analysis using generalized power series: Part I—Theory," to be published.

[12] M. B Steer and G. W. Rhyne, "Frequency domain nonlinear circuit analysis using generalized power series: Part II—Application," to be published.

[13] M. B. Steer, P. J. Khan, and R. S. Tucker, "Relationship of Volterra series and generalized power series," *Proc. IEEE*, pp. 1453–1454, Dec. 1983.

[14] G. L. Heiter, "Characterization of nonlinearities in microwave devices and systems," *IEEE Trans. Microwave Theory Tech.*, vol. MTT-21, pp. 797–805, Dec. 1973.

[15] R. S. Tucker and C. Rauscher, "Modelling the 3rd-order intermodulation-distortion properties of a GaAs F.E.T.," *Electron. Lett.*, vol. 13, pp. 508–509, Aug. 18, 1977.
[16] M. B. Steer and P. J. Khan, "An algebraic formula for the complex output of a system with multi-frequency excitation," *Proc. IEEE*, pp. 177–179, Jan. 1983.
[17] G. W. Rhyne and M. B. Steer, "Simulation of intermodulation distortion in MESFET circuits with arbitrary frequency separation of tones," in *IEEE MTT-S Int. Microwave Symp. Dig.*, 1986, pp. 547–550.
[18] A. Materka and T. Kacprzak, "Computer calculation of large-signal GaAs FET amplifier characteristics," *IEEE Trans. Microwave Theory Tech.*, vol. MTT-33, pp. 129–135, Feb. 1985.
[19] D. L. Peterson, A. M. Pavio, Jr., and B. Kim, "A GaAs FET model for large-signal applications," *IEEE Trans. Microwave Theory Tech.*, vol. MTT-32, pp. 276–281, Mar. 1984.
[20] TOUCHSTONE, EEsof Inc., Westlake Village, CA.
[21] C. Rauscher and H. A. Willing, "Simulation of nonlinear microwave FET performance using a quasi-static model," *IEEE Trans. Microwave Theory Tech.*, vol. MTT-27, pp. 834–840, Oct. 1979.
[22] W. R. Curtice and R. L. Camisa, "Self-consistent GaAs FET models for amplifier design and device diagnostics," *IEEE Trans. Microwave Theory Tech.*, vol. MTT-32, pp. 1573–1578, Dec. 1984.
[23] F. Diamond and M. Laviron, "Measurement of the extrinsic series elements of a microwave MESFET under zero current conditions," in *Proc. 12th European Microwave Conf.*, Sept. 1982.

George W. Rhyne (S'87) received the B.S. and M.S. degrees in electrical engineering from North Carolina State University in 1982 and 1985, respectively. He is currently completing the Ph.D. degree at North Carolina State University. His research interests are in the areas of nonlinear circuit analysis, the computer-aided design and testing of microwave circuits, and the characterization of microwave devices.

✠

Michael B. Steer (S'78–M'82) received the Ph.D. degree in electrical engineering from the University of Queensland, Brisbane, Australia, in 1983 and is currently Assistant Professor of Electrical and Computer Engineering at North Carolina State University. His research involves the simulation and computer-aided design of nonlinear analog circuits with large-signal excitation and of circuits with mixed analog and digital signals. Dr. Steer is currently working on the simulation of microwave analog circuits, delta-sigma modulators, high-speed printed circuit boards, and local area networks. In 1987 he was named a Presidential Young Investigator.